Modelling and Precalculation of Additional Losses of Inverter Fed Asynchronous Induction Machines for Traction Applications

F. Müllner, H. Neudorfer
Traktionssysteme Austria, Wiener Neudorf, Austria
florian.muellner@traktionssysteme.at

E. Schmidt, *Member, IEEE*
Institute of Energy Systems and Electric Drives
Vienna University of Technology, Vienna, Austria

***Abstract* - The inverter supply of asynchronous induction machines for traction applications has a major influence on both electromagnetic and thermal performance. In addition asynchronous induction machines used with traction drives of rail transportation vehicles have different design strategies compared against commonly used standard machines. Generally, the design of these machines requires high electromagnetic and thermal stress. Thus, the additional losses caused by the inverter have to be considered with the initial design. Concerning the thermal design, a precalculation of the additional losses at various operating points is necessary. The additional losses depend on the characteristics of the machine as well as on the operating mode of the inverter. DC-link voltage and switching frequency have major effects on the additional losses. An important viewpoint of modelling and precalculation presented herein is given to the comparison with detailed measurements from different already built machines. Furthermore, the precalculation of additional losses enables the determination of an optimized switching mode to minimize the losses in the system of inverter and induction machine.**

***Index Terms* - Additional losses, Traction drive, Inverter-fed machines, Induction machine, Asynchronous machine**

I. INTRODUCTION

The evaluation of additional losses of inverter fed induction machines is an important task for many years, but losses are mainly investigated with commonly used standard machines. Compared with industrial utilized machines, design and manufacturing cycles of induction machines used with traction drives are mostly very different. Therefore, accurate modelling and pre-evaluation of the additional losses caused by the inverter are very important tasks in particular during the initial design and tender phase. In these design phases, many details of both machine and inverter, in particular operating and switching strategies have not been specified. Consequently, very detailed analysis methods such as multi-domain coupled finite element analyses are not advisable. In contrast, analytical calculations will be used in order to fulfil the requirements.

The presented calculation bases on a machine model concerning the higher harmonics and a simulation of the traction converter. Equivalent circuits of the induction machine for each higher harmonic component of the terminal voltages applied by the inverter are utilized to calculate the higher harmonic components of the current consumption. Subsequently, the iron and power losses are evaluated in dependence on the operating conditions particularly taking into account the various switching strategies of the inverter. Based on detailed measurement data from already built machines, a fast and reliable calculation method of the additional losses suitable for the initial design of new machines is presented.

II. EQUIVALENT CIRCUITS

The voltages applied to the machine and consequently the consumed currents are always non-sinusoidal with dominant fundamental harmonic components U_1, I_1 and various higher harmonic components U_k, I_k. In the case of a synchronous pulse pattern, harmonic orders are determined by $k = 1 + 6g$, $g \in Z$. In contrast an asynchronous pulse pattern leads to harmonic orders

$$k = n\frac{f_s}{f_1} \pm m, \quad n, m \in N \tag{1}$$

which are not an integer, but related to the switching frequency f_s and the fundamental frequency f_1. Based on

Fourier series expansions of voltages and currents, an equivalent circuit of each harmonic order k as shown in Fig. 1 is introduced. The slip values s_k of the higher harmonics are obtained from the fundamental slip s_1 as

$$1 - s_1 = k(1 - s_k) \; . \tag{2}$$

With rated operational conditions, the fundamental slip $s_1 \ll 1$ causes slip values of the higher harmonics $s_k \approx 1$. Consequently, the higher harmonics will generate additional losses which are approximately independent of the actual operational point [1], [2]. The parameters of each equivalent circuit are further calculated according to the following suggestions about power and iron losses.

III. Additional Losses

A. Power losses

The most important component of the additional losses concerned arises as power losses from higher current harmonics in the conductors of both stator and rotor windings [2], [3]. Due to the high frequencies of these current components, the current displacement effects have to be considered in detail. Based on the well-known skin depth

$$\delta_C = \sqrt{\frac{2}{\omega \mu_0 \gamma}} \tag{3}$$

in dependence on circular frequency ω and conductivity γ [2], [4], [5], a modified reduced slot height ξ considering the insulation of the conductor is defined as

$$\xi = \frac{h_C}{\delta_C} \sqrt{\frac{b_C}{b_S}} \tag{4}$$

where h_C, b_C, b_S denote the height of the conductor as well as the total width of conductors and width of slot, respectively. Additionally a complex parameter ζ is defined as

$$\zeta = \xi(1 + j) \, . \tag{5}$$

The skin effect significantly affects the impedance of slot conductors along the lengths of stator and rotor lamination stack. In particular with the stator, the current displacement within the end winding region has to be considered, too [4].

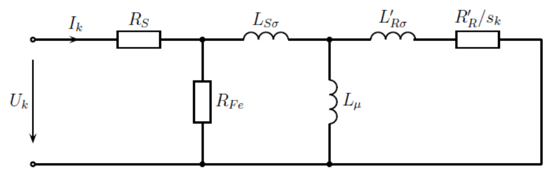

Fig. 1: Equivalent circuit for each harmonic component

Asynchronous induction machines of traction drives are always equipped with opened stator slots in order to carry the form-wound winding coils [6], [7]. Furthermore, in most cases, asynchronous induction machines of traction drives are equipped with unskewed semiclosed rotor slots containing rectangular or slightly trapezoidal slot conductors. Therefore, precalculation of additional losses has to keep in mind some fundamental differences compared with industrial utilized machines.

B. Opened stator slots

Usually, there is an equal number of rectangular conductors in both upper and lower layer resulting in an even number n of slot conductors. By using DC resistance R_0 and DC inductance L_0 [5], the complex impedance of each of the n rectangular slot conductors is given by

$$\frac{Z(\zeta)}{R_0} = \zeta \left(\coth \zeta + 2p(p-1) \tanh \frac{\zeta}{2} \right) \, , \;\; 1 \le p \le n \; . \tag{6}$$

The decomposition into real and imaginary parts yields

$$k_{pR}(\xi) = \frac{\operatorname{Re} Z(\zeta)}{R_0} = \varphi_R(\xi) + p(p-1)\psi_R(\xi) \;\; , \tag{7}$$

$$k_{pX}(\xi) = \frac{\operatorname{Im} Z(\zeta)}{\omega L_0} = \varphi_X(\xi) + p(p-1)\psi_X(\xi) \;\; , \tag{8}$$

with the real functions

$$\varphi_R(\xi) = \xi \frac{\sinh 2\xi + \sin 2\xi}{\cosh 2\xi - \cos 2\xi} \;\; , \tag{9}$$

$$\psi_R(\xi) = 2\xi \frac{\sinh \xi - \sin \xi}{\cosh \xi + \cos \xi} \;\; , \tag{10}$$

$$\varphi_X(\xi) = \frac{3}{2\xi} \frac{\sinh 2\xi - \sin 2\xi}{\cosh 2\xi - \cos 2\xi} \;\; , \tag{11}$$

$$\psi_X(\xi) = \frac{3}{\xi} \frac{\sinh \xi + \sin \xi}{\cosh \xi + \cos \xi} \;\; . \tag{12}$$

In dependence on the arrangement of the slot conductors with the end winding connection, averaged values of resistance and inductance are described as

$$k_{nR}(\xi) = \varphi_R(\xi) + m(n)\psi_R(\xi) \;\; , \tag{13}$$

$$k_{nX}(\xi) = \frac{1}{n^2}\left(\varphi_X(\xi) + m(n)\psi_X(\xi)\right) \;\; . \tag{14}$$

Therein, weighting factors

$$m(n) = \frac{n^2 - 1}{3} \;\; , \quad m(n) = \frac{n^2 - 4}{6} \tag{15}$$

are introduced without or with transposition of the $n/2$ slot conductors in each layer, respectively [4].

In particular with the stator, the current displacement within the end winding region has to be considered. According to [2], [4], the modified reduced conductor height

$$\xi' = \frac{h_C}{\delta_C}\sqrt{\frac{b_C}{b_C + 0.6nh_C}} \tag{16}$$

and modified weighting factor

$$m'(n) = \frac{n^2 - 4}{12} \tag{17}$$

define the averaged values of resistance and inductance as

$$k'_{nR}(\xi') = \varphi_R(\xi') + m'(n)\psi_R(\xi') \ , \tag{18}$$

$$k'_{nX}(\xi') = \frac{4}{n^2}(\varphi_X(\xi') + m'(n)\psi_X(\xi')) \ . \tag{19}$$

Finally, averaged resistance and inductance factors are obtained from

$$k_R(\xi) = \frac{k_{nR}(\xi)l_S + k'_{nR}(\xi')(l_W - l_S)}{l_W} \tag{20}$$

$$k_X(\xi) = \frac{k_{nX}(\xi)l_S + k'_{nX}(\xi')(l_W - l_S)}{l_W} \tag{21}$$

wherein l_S and l_W denotes stacking length and half total length of one single winding, respectively.

C. Semi-closed rotor slots

By using the DC resistance R_0, the complex impedance of rectangular slot conductors is given by

$$\frac{Z(\zeta)}{R_0} = \zeta^2\left(\frac{\coth\zeta}{\zeta} + \sum_{n=1}^{\infty} 2\left(si\,\frac{n\pi s}{b_C}\right)^2 \frac{\coth\zeta_n}{\zeta_n}\right) \ , \tag{22}$$

$$\zeta_n = \sqrt{\left(\frac{2n\pi h_C}{b_C}\right)^2 + \zeta^2} \ ,$$

where s, b_C, h_C denote width of the slot opening as well as width and height of the conductor, respectively [5].

With respect to the additional losses of the higher harmonics, the impact of various designs of the end winding region can be neglected.

D. Iron losses

Another important component of the additional losses arises as iron losses caused by the higher voltage harmonics in particular in the stator and less significantly in the rotor laminations [2], [3]. Basically, iron losses can be separated into three contributions of eddy current losses P_{ed}, hysteresis losses P_{hyst} and excess losses P_{exc} [8] - [13]. Each of these three iron loss densities has its own dependence on frequency and magnetic flux:

$$p_{ed} \sim f_k^2\left(\frac{U_k}{f_k}\right)^2 \ , \tag{23}$$

$$p_{hyst} \sim f_k\left(\frac{U_k}{f_k}\right)^2 \ , \tag{24}$$

$$p_{exc} \sim f_k^{1.5}\left(\frac{U_k}{f_k}\right)^{1.5} \ . \tag{25}$$

The pulse pattern applied by the inverter has an effect on the hysteresis losses because appearance of minor hysteresis loops has to be considered [13]. Furthermore, the hysteresis losses are additionally influenced by the level of saturation caused by the fundamental harmonics [11].

The magnetizing inductance of the fundamental harmonics can be evaluated in accordance with the magnetic characteristic of the entire machine for each operating point in either the constant field or field weakening region. Additionally, the saturation caused by the fundamental component defines an appropriate differential magnetizing inductance representing the magnetization current of the higher harmonics. The actual values of the iron losses are obtained from the geometry data as well as material dependent coefficients known from already utilized lamination sheets. According to four main iron regions as stator teeth and yoke as well as rotor teeth and yoke, the total iron losses of these regions are evaluated from the above power loss densities and the iron masses of the respective regions.

IV. Comparison with Measurements

Fig. 2 depicts the measurement data for the additional losses caused by the inverter for a typical traction machine in dependence of the switching frequency at a constant DC link voltage. Accordingly, Fig. 3 and Fig. 4 depict the simulation data for the additional losses caused by the inverter at a constant value of the DC link voltage, calculated with different switching frequencies of the inverter. A comparison of Fig. 3 and Fig. 4 shows that especially power losses in the rotor are highly influenced by the switching frequency. Furthermore, relative distribution of additional losses within the machine changes strongly with different switching frequencies.

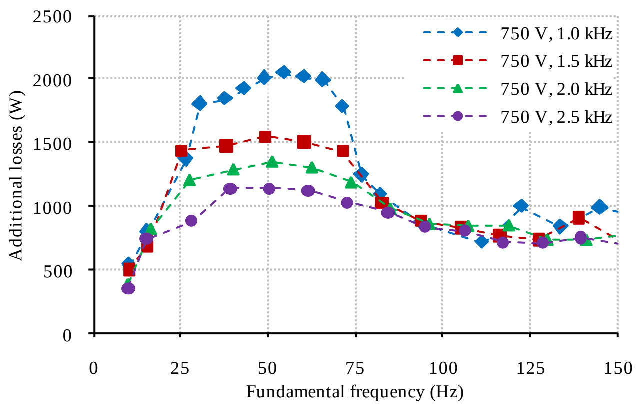

Fig. 2: Measurement data of additional losses caused by the inverter for an induction machine of traction drives with a rated power of 100 kW in dependence on the switching frequency, DC link voltage of 750 V

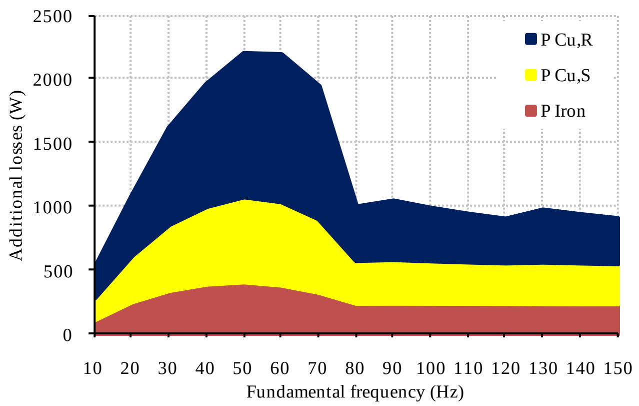

Fig. 3: Simulated main components of additional losses caused by the inverter for an induction machine of traction drives with a rated power of 100 kW, switching frequency of 1 kHz, DC link voltage of 750 V

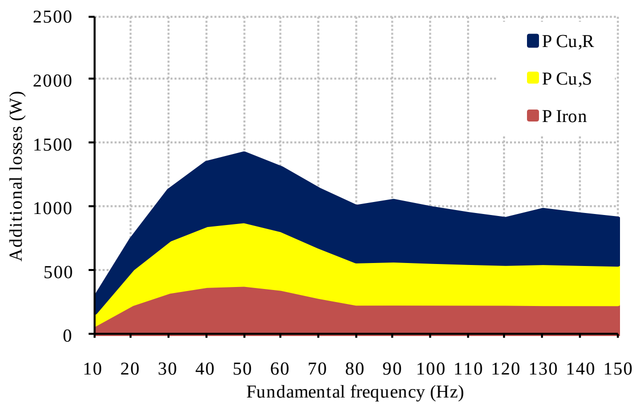

Fig. 4: Simulated main components of additional losses caused by the inverter for an induction machine of traction drives with a rated power of 100 kW, switching frequency of 2 kHz, DC link voltage of 750 V

As obtained from measurements, the switching frequency of the inverter significantly affects the total additional losses caused by the higher harmonic components. On the other hand, an increased switching frequency of the inverter causes additional losses and subsequently thermal design problems with the inverter. Additionally, the DC link voltage strongly influences the total additional losses caused by the higher harmonic components since these losses depend on the DC link voltage approximately quadratic.

The comparison with the evaluated data obtained from equivalent circuits of the higher harmonics shows a good accordance. As expected, the most dominant part of the additional losses caused by the higher harmonics arises from the power losses within the rotor. All three main components of the additional losses increase with fundamental frequencies up to values which approximately equal half of the highest frequency in the constant field region. With higher fundamental frequencies in the upper constant field region, they decrease to smaller values. Finally, all three portions are approximately constant within the field weakening region. The level and the characteristics of the additional losses in the field weakening region are mainly influenced by the pulse pattern of the inverter.

V. System Efficiency

As a consequence, there are important fields of an optimization of both electrical machine and inverter in order to get an optimal behaviour of the system in terms of losses and efficiency. Beside optimisation of losses other implications of the pulse pattern should be considered too, e.g. dielectric stress and radiated noise. In order to reduce the additional losses caused by the inverter, in particular switching mode as well as DC link voltage of the inverter should be selected for each application separately.

A. Switching frequency

Fig. 5 depicts the additional losses caused by the inverter in dependence of switching frequency at frequencies up to 6 kHz at different values of DC link voltage. In general, the higher the switching frequency, the lower the total additional losses caused by the inverter. The distribution of additional losses in stator losses and rotor losses as well as in power losses and iron losses depends on the switching mode as mentioned above. Furthermore, additional losses are depending on the operating point, thus the optimal switching mode depends on the respective operating point.

The losses in the inverter can be separated mainly into conduction losses and switching losses whereat primarily switching losses are influenced by the switching mode. In order to describe the losses in the inverter, the switching mode is mainly characterized by the switching frequency. Therefore, comparing the switching losses of the inverter with the additional losses of the machine leads to a switching frequency with minimal losses in the system. Consequential, a switching mode with minimal losses in the system can be determined as depicted in Fig. 6.

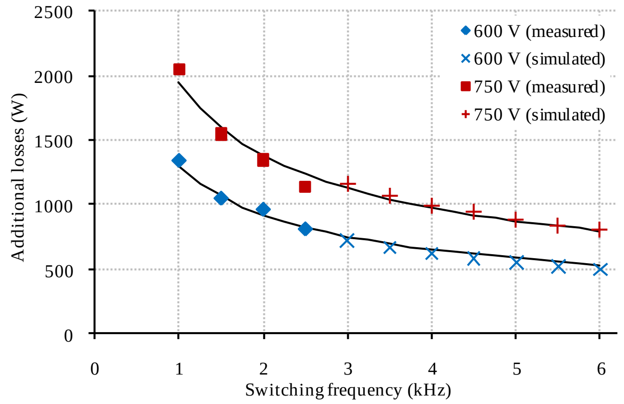

Fig. 5: Measured and simulated data of additional losses for an induction machine with a rated power of 100 kW in dependence on the switching frequency at two different values of DC link voltage

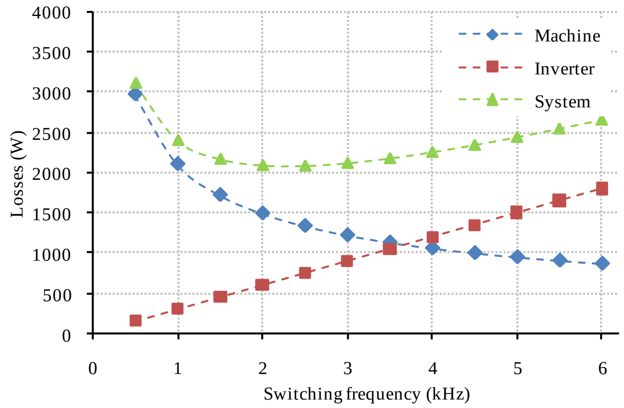

Fig. 6: Comparison of losses of the electrical machine and switching losses of the inverter

B. *Pulse pattern*

In the field weakening region either a synchronous or an asynchronous pulse pattern is an appropriate switching mode. Applying a synchronous pattern leads at higher fundamental frequencies to a higher switching frequency according to a constant number of cycles per fundamental period. Therefore additional losses decrease with higher fundamental frequency. In contrast, using an asynchronous pattern with a constant switching frequency implies increasing additional losses with increasing fundamental frequency caused by high voltage harmonics at a low number of cycles per fundamental period. Fig. 7 depicts the simulated data of additional losses using different switching modes in the field weakening region. The asynchronous pulse pattern was simulated with a constant switching frequency of 2 kHz. Simulation of synchronous pulse pattern was done with a switching frequency of 1.95 kHz at maximum fundamental frequency. Therefore, switching frequency with the synchronous pulse pattern is in the entire operating range lower compared to the asynchronous pulse pattern. As a result of optimization of the synchronous pulse pattern, this switching mode is capable to work at lower additional losses of the motor and lower switching losses of the inverter than an asynchronous pulse pattern. In contrast, especially with a synchronous pulse pattern radiated noise and circuit feedback have to be considered in detail. The optimal pulse pattern is dependent on the characteristics of both induction machine and inverter as well as on the operating point.

C. *DC link voltage*

Usually an asynchronous pulse pattern is used in the constant field region. Therefore, the level of additional losses can be mainly influenced by switching frequency and DC link voltage. Maximum switching frequency is often limited by the thermal design of the inverter because of switching losses. Hence, a minimization of additional losses would require a variable DC link voltage in the constant field region. Fig. 8 shows the possibility of loss minimization with usage of a variable DC link voltage. The simulation at constant link voltage was done with 750 V. In the case of variable link voltage the DC link voltage was varied between 600 V and 750 V, the fundamental voltage remained unchanged in the entire operating range.

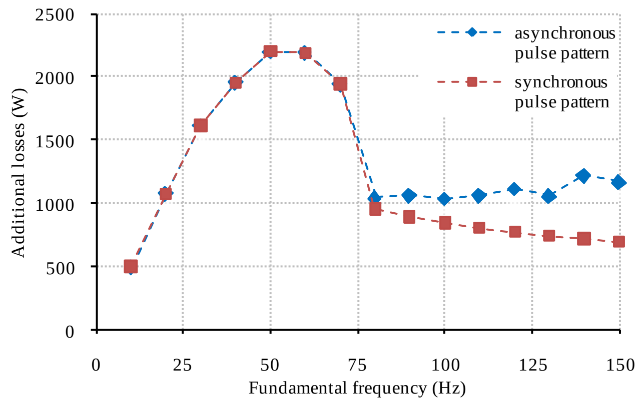

Fig. 7: Additional losses caused by the inverter using different switching modes in the field weakening region

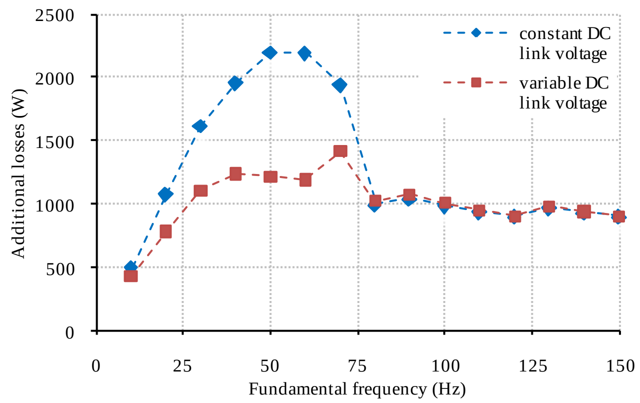

Fig. 8: Additional losses caused by the inverter, comparison of constant and variable DC link voltage in the constant field region, constant switching frequency of 1 kHz

VI. CONCLUSION

In terms of additional losses caused by non-sinusoidal voltages and currents of the supplying voltage source inverter, asynchronous induction machines used with traction drives of rail transportation vehicles have to be treated differently than standard induction machines. Therefore, the paper discusses modelling and precalculation of power and iron losses additionally arising from the inverter to be suitable for a more accurate initial design of such machines.

Special attention is paid to an inclusion of various components of the iron losses as well as an accurate evaluation of the current displacement and the subsequent additional power losses in both stator and rotor slot conductors including the end winding regions. The presented evaluation method based on Fourier analyses of the terminal voltages is successfully compared with detailed measurement results obtained from already built machines.

Simulation of additional losses caused by the inverter enables a detailed study on system efficiency. Thus, minimization of losses in the system of induction machine and inverter is evaluated by comparing different switching modes of the inverter in the constant field region as well as in the field weakening region. In addition, the consequence of a variable DC link voltage applied in the constant field region is analyzed.

REFERENCES

[1] Kleinrath H.: Stromrichtergespeiste Drehfeldmaschinen (in German), Springer, Vienna, 1980.

[2] Pyrhönen J., Jokinen T., Hrabovcová V.: Design of Rotating Electrical Machines, John Wiley & Sons Ltd, Chicester (UK), 2008.

[3] Green T.C., Hernandez-Aramburo C.A., Smith A.C.: "Losses in Grid and Inverter Supplied Induction Machine Drives", IEE Proceedings Electrical Power Applications, Vol. 150, No. 6, November 2003.

[4] Müller G., Vogt K., Ponick B.: Berechnung elektrischer Maschinen (in German), Wiley-VCH, Weinheim, 2008.

[5] Schmidt E.: Stromverdrängung in Nutenleitern (in German), Master Thesis, Vienna University of Technology, 1985.

[6] Islam M.J., Arkkio A.: "Effects of Pulse-Width Modulated Supply Voltage on Eddy Currents in the Form-Wound Stator Winding of a Cage Induction Motor", IET Electric Power Applications, Vol. 3, No. 1, January 2009.

[7] Islam M.J., Khang H.V., Repo A.K., Arkkio A.: "Eddy Current Loss and Temperature Rise in the Form-Wound Stator Winding of an Inverter Fed Cage Induction Motor", IEEE Transaction on Magnetics, Vol. 46, No. 8, August 2010.

[8] Boglietti A., Bottauscio O., Chiampi M., Pastorelli M., Repetto M.: "Computation and Measurement of Iron Losses under PWM supply conditions", IEEE Transactions on Magnetics, Vol. 34, No. 4, July 1998.

[9] Boglietti A., Chiampi M., Repetto M., Bottauscio O., Chiarabaglio D.: "Loss Separation Analysis in Ferromagnetic Sheets Under PWM Inverter Supply", IEEE Transactions on Magnetics, Vol. 34, No. 4, July 1998.

[10] Pippuri J., Arkkio A.: "Time-Harmonic Induction Machine Model Including Hysteresis and Eddy Currents in Steel Laminations", IEEE Transaction on Magnetics, Vol. 45, No. 7, July 2009.

[11] Boglietti A., Cavagnino A., Ionel D.M.. Popescu M., Staton D.A., Vaschetto S.: "A General Model to Predict the Iron Losses in PWM Inverter-Fed Induction Motors", IEEE Transactions on Industry Applications, Vol. 46, No. 5, September 2010.

[12] Krings A., Soulard J.: "Overview and Comparison of Iron Loss Models for Electrical Machines", Journal of Electrical Engineering, Vol. 10, No. 3, September 2010.

[13] Dlala E., Arkkio A.: "A General Model for Investigating the Effects of the Frequency Converter on the Magnetic Iron Losses of a Squirrel-Cage Induction Motor", IEEE Transactions on Magnetics, Vol. 45, No. 9, September 2009.